Supporting Information

Chemical, Radiochemical and Biological Studies of New Gallium(III) Complexes with Hexadentate Chelators

Francisco Silva[1], Maria Paula C. Campello[1], Lurdes Gano[1], Célia Fernandes[1], Isabel C. Santos[1], Isabel Santos[1], José R. Ascenso[2], M. João Ferreira[2], António Paulo[1,*]

[1]*Centro de Ciências e Tecnologias e Nucleares, IST, Universidade de Lisboa, Estrada Nacional 10, 2695-066 Bobadela LRS, Portugal*

[2]*Centro de Quimica Estrutural, IST, Universidade de Lisboa, Avenida Rovisco Pais 1, 1049-001, Lisboa, Portugal*

Synthesis

Synthesis of [GaL^{pz*,OMe}](ClO$_4$): To a solution of $Ga(NO_3)_3.10H_2O$ (111 mg, 0.26 mmol) in MeOH (5 mL) was added dropwise a solution of **H$_2$L$^{pz*,C=N}$** (130 mg, 0.32 mmol) also in MeOH (5 mL). To the resulting clear solution, was added $NaCH_3COO.3H_2O$ (87 mg, 0.64 mmol) dissolved in 5 mL of MeOH, and the reaction mixture was stirred overnight at room temperature. Then, the mixture was treated with $NaClO_4.H_2O$ (44 mg, 0.31 mmol) and was let to stand in the refrigerator. After several days, a white crystalline solid precipitated, which was formulated as **[GaL^{pz*,OMe}](ClO$_4$)** (Scheme S1). Yield: 65 mg (36%).

Anal. Calcd for $C_{26}H_{32}N_5O_7ClGa.CH_3OH$ (662.15): C, 48.85; H, 5.47; N, 10.55. found: C, 48.02; H, 5.38; N, 10.52. ESI-MS: m/z calcd for $[M]^+$, 532.2; found 532.2. IR (KBr, ν/cm^{-1}) 3379m (N-H), 3229mw, 2928w, 1643s (N=C), 1603m, 1551m, 1472sh,m, 1455s, 1306s, 1084s (C-O) , 975mw, 894m, 858mw, 752m, 622m, 607sh,m, 534w, 472w, 414w. 1084 (C-O). ^{1}H NMR (293K, 500 MHz, CD_3CN) δ_H 1.99 (3H, s, CH_3), 2.36 (3H, s, CH_3), 2.46 (1H, m, CH_2), 2.67 (1+1H, m, CH_2), 2.78 (1H, dd, CH_2), 2.98 (1H, m, CH_2), 3.11 (1H, m, CH_2), 3.15 (3H, s, OCH_3), 3.22 (1H, m, CH_2), 3.52 (1H, m, CH_2), 3.63 (1H, m, CH_2), 4.09 (1H, d, NH), 4.22 (1H, d, CH_2), 4.92 (1H, tr, CH_2), 5.49 (1H, s, CH), 6.07 (1H, s, H(4)-pz), 6.63 (1H, d, Ph), 6.71 (1H, tr, Ph), 6.81-6.87 (1+1H, m, Ph), 7.18 (1H, tr, Ph), 7.35 (1H, d, Ph), 7.41-7.47 (1+1H, m), 8.54 (1H, s, CH=N); ^{13}C NMR (293K, 125 MHz, CD_3CN) δ_C10.927 (CH_3), 12.36 (CH_3), 35.07 (CH_2), 43.31 (CH_2), 51.80 (CH_2), 53.03 (CH_2), 53.50 (CH_2), 56.68 (OCH_3), 57.75 (CH_2), 88.46 (CH), 107.41 (C(4)-pz), 116.80 (Ph), 119.18 (Ph), 122.39 (Ph), 122.93 (Ph), 127.93 (Ph), 130.88 (Ph), 135.49

(Ph), 136.61 (Ph), 143.70 (C(5)-pz), 150.41 (C(3)-pz, 160.65 (Ph), 166.83 (Ph), 171.64 (CH=N); ^{71}Ga NMR (293K, 152MHz, CD_3CN) δ_{Ga} 68; ^{15}N NMR (293K, 51MHz, CD_3CN) : δ_N44.9 (NH).

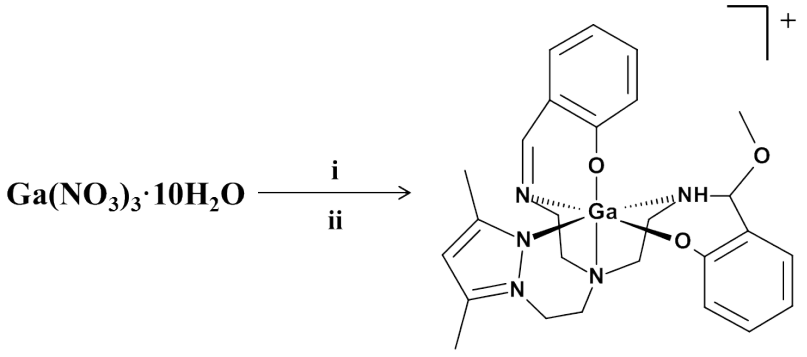

Scheme S1. Synthesis of **[GaL^{pz*,OMe}]$^+$.** i) $H_2L^{pz*,C=N}$, $NaCH_3COO$, MeOH, r.t., o.n.; ii) $NaClO_4$.

[GaL^{1,OMe}](ClO$_4$) was further characterized by X-ray diffraction analysis (Tables S1 and S2 and Fig. S1) and by bidimensional NMR techniques (S4, S5 and S6), which allowed the assignments of the several resonances in the ^{1}H NMR spectrum of the complex (Fig. S2). The NMR studies confirmed that its molecular structure in solution corresponds to the one found in the solid state, i.e. a structure containing a coordinated pyrazolyl in an axial position *trans* to the NH group with the two phenoxide oxygens bound to the metal in *cis*-*cis* positions relative to the pyrazolyl ring.

X-ray crystallography data

Table S1: Crystallographic details for **[GaL^{pz*,OMe}](ClO$_4$)**

[GaL^{pz*,OMe}](ClO$_4$).(MeOH)	
empirical form.	$C_{27}H_{37}N_5O_8ClGa$
f_w	664.79
temp. (K)	150(2)
cryst. system	triclinic
space group	P-1
a (Å)	8.3515(2)
b (Å)	9.8243(3)
c (Å)	18.2097(5)
α (deg)	78.347(1)
β (deg)	80.943(1)
γ (deg)	86.333(2)
V (Å^3)	1444.23(7)
Z, D_{calcd} (Mg/m^3)	2,1.529
μ (mm^{-1})	1.104
F(000)	692
θ range (deg)	3.12-25.03
h,k,l range	-9/9,-11/11,-21/20
reflns col./uniq.	15192/5017 [Rint=0.0634]
T max./min.	0.9676/0.8095
S on F^2	0.973
R1 (I > 2σ(I))	0.0437
wR2 (all data)	0.1121

[a]Definitions: $R1 = \sum||F_o| - |F_c||/\sum|F_o|$, $wR2 = [\sum w(F_o^2 - F_c^2)^2/\sum w(F_o^2)^2]^{1/2}$

Table S2. Selected Bond Lengths (Å) and Angles (º) for **[GaL^{pz*,OMe}](ClO$_4$)**

[GaL^{pz*,OMe}](ClO$_4$).(MeOH)			
Ga1-O1	1. 908(2)	Ga1-N2	2.185(3)
Ga1-N3	2.042(3)	Ga1-O2	1. 902(2)
Ga1-N4	2.099(3)	Ga1-N1	2.135(3)
O1-Ga1-O2	92.20(10)	O1-Ga1-N1	90.77(10)
O2-Ga1-N1	91.10(11)	O1-Ga1-N4	85.86(10)
O2-Ga1-N4	101.14(11)	N1-Ga1-N4	167.40(11)
O1-Ga1-N3	172.86(11)	O2-Ga1-N3	89.95(11)
N1-Ga1-N3	96.00(11)	N4-Ga1-N3	87.04(11)
O1-Ga1-N2	98.12(10)	O2-Ga1-N2	165.87(10)
N1-Ga1-N2	79.19(11)	N4-Ga1-N2	89.26(11)
N3-Ga1-N2	80.99(11)		

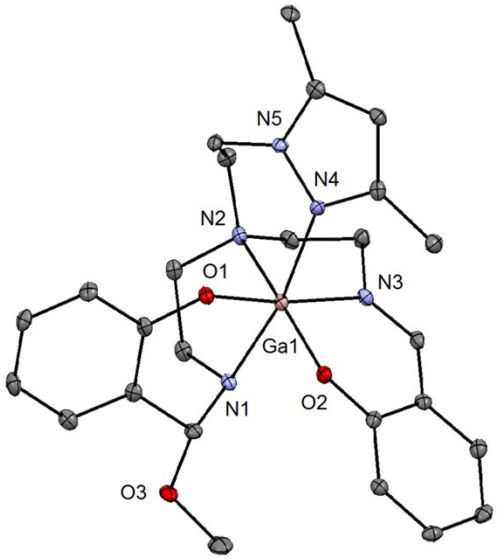

Figure S1. ORTEP drawing at the 40% probability level for the **[GaL^{pz*,OMe}]$^{+}$** cation in **[GaL^{pz*,OMe}]ClO$_4$**. Hydrogen atoms are omitted for clarity.

NMR data

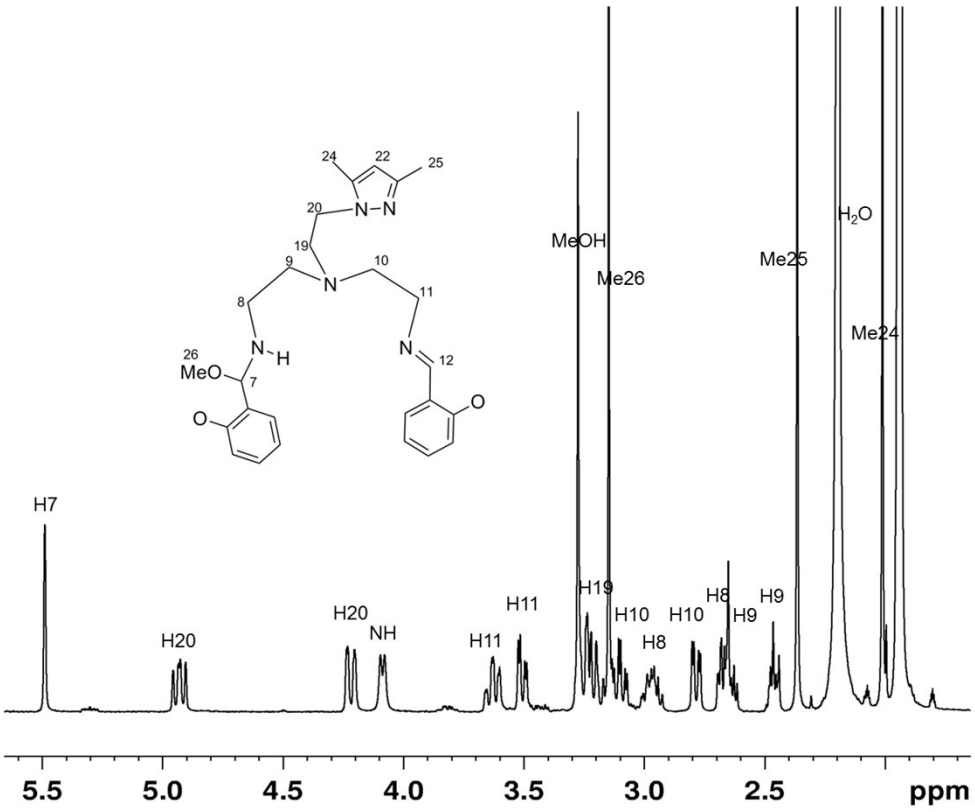

Figure S2. Aliphatic region of the ^{1}H spectrum of **[GaL^{pz*,OMe}](ClO$_4$)** in CD_3CN showing the assignment of methylenic protons. Methyl groups of the pyrazolyl ring and amine NH proton are also identified. Peaks from residual solvents (MeOH and H_2O) are also assigned.

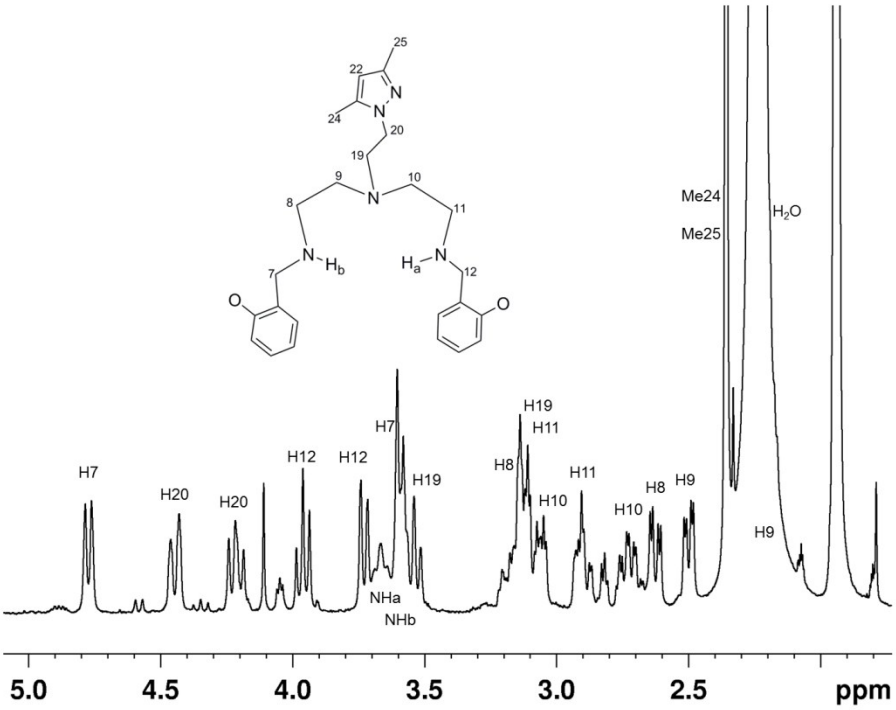

Figure S3. Aliphatic region of the ^{1}H spectrum of **[GaL^{pz*,NH}](ClO$_4$)** in CD_3CN showing the assignment of methylenic protons. Methyl groups of the pyrazolyl ring and amine NH protons are also identified. Peak from residual water is also assigned.

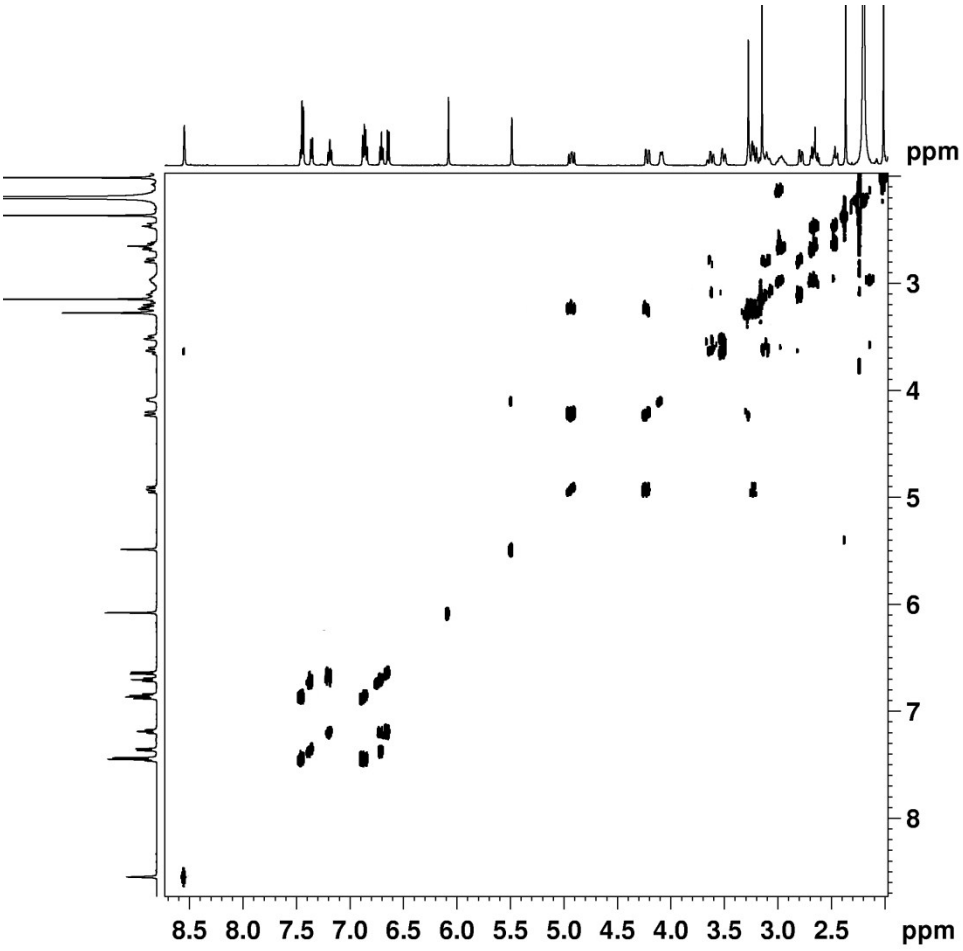

Figure S4. COSY spectrum of [**GaL**$^{\mathbf{pz*,OMe}}$]$^{+}$ in CD_3CN.

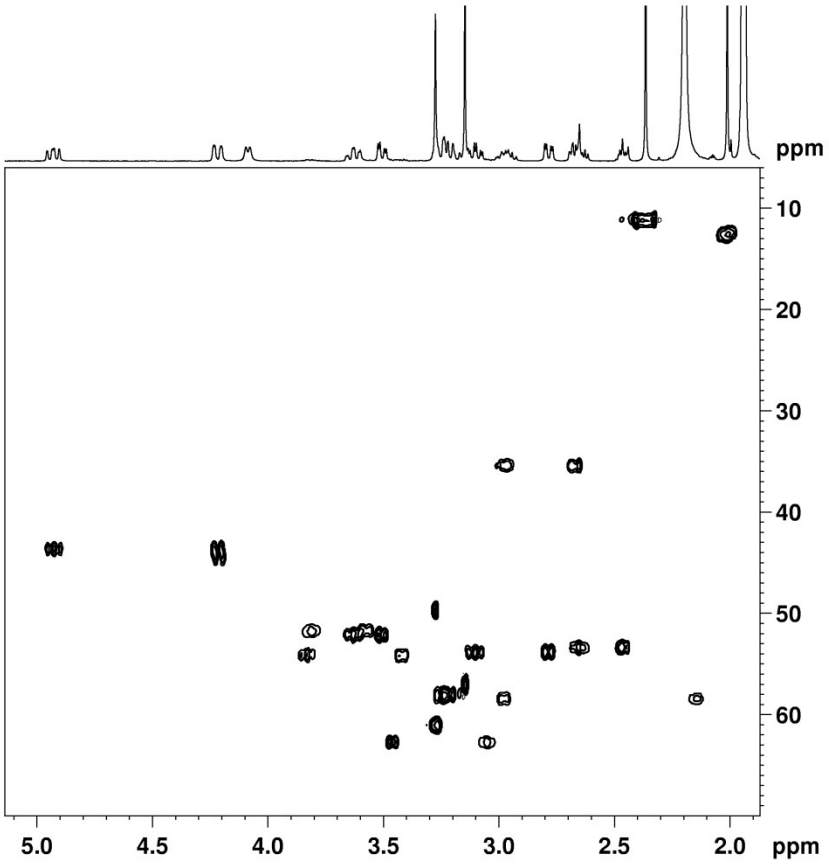

Figure S5. HSQC spectrum of aliphatic carbons of [**GaL^{pz*,OMe}](ClO$_4$)** in CD_3CN.

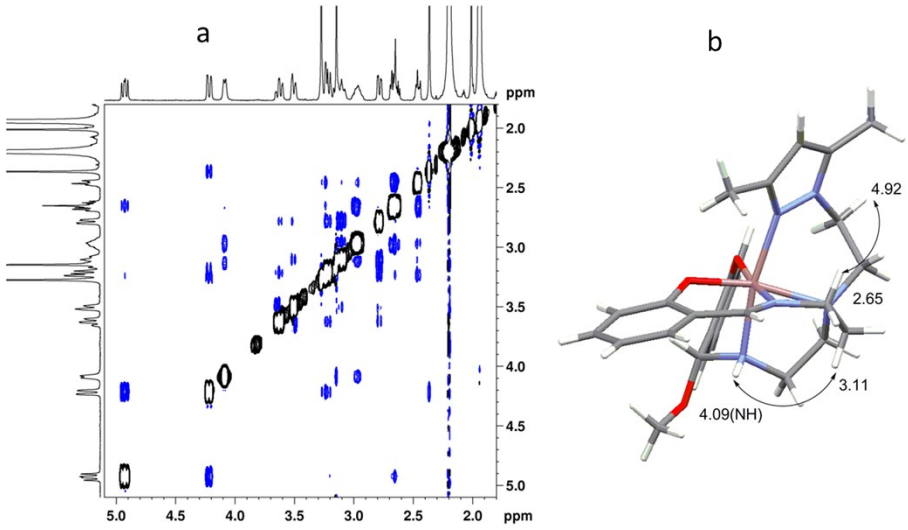

Figure S6. a) Aliphatic region of the NOESY spectrum of **[GaL^{pz*,OMe}](ClO$_4$)** in CD_3CN; **b)** Relevant NOE enhancements used to confirm the *cis-cis* coordination of **L^1**.

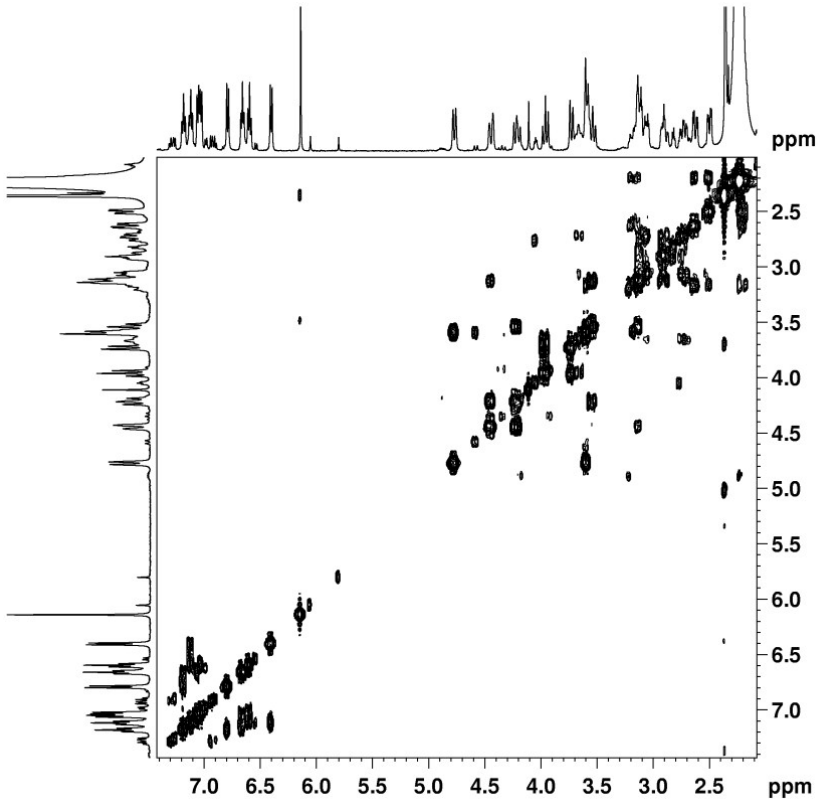

Figure S7. COSY spectrum of [**GaL^{pz*,NH}](ClO$_4$)** in CD_3CN.

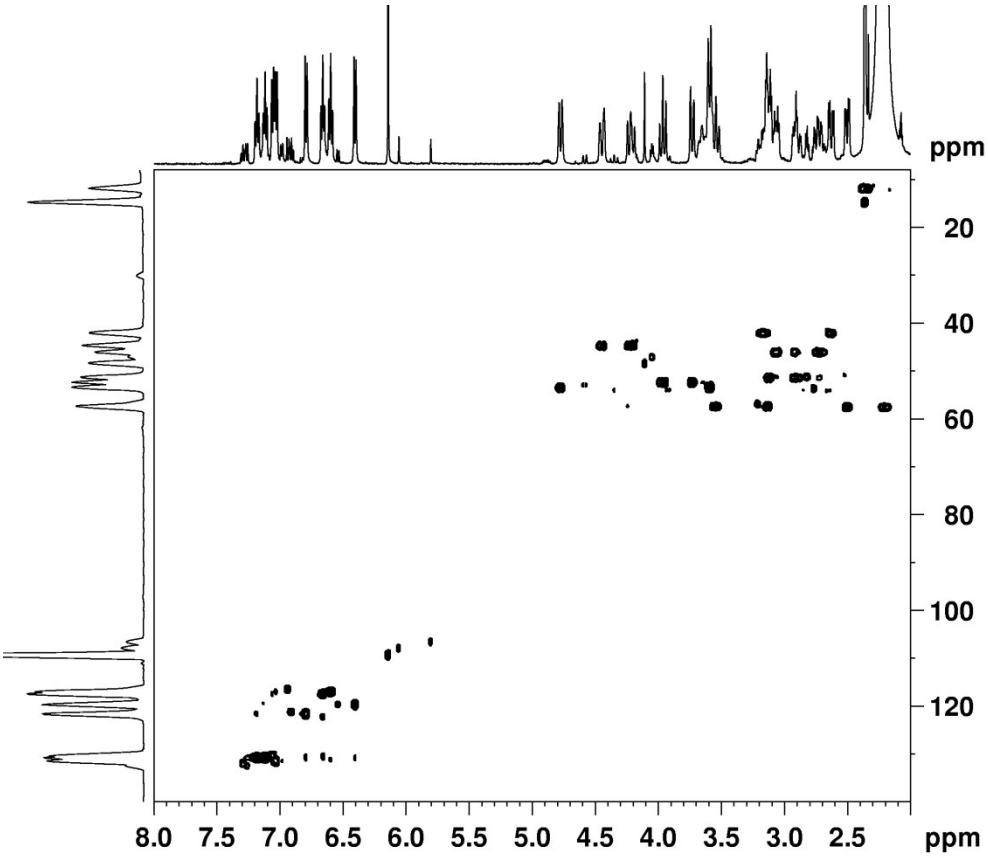

Figure S8. HSQC spectrum of [**GaL^{pz*,NH}](ClO$_4$)** in CD_3CN.

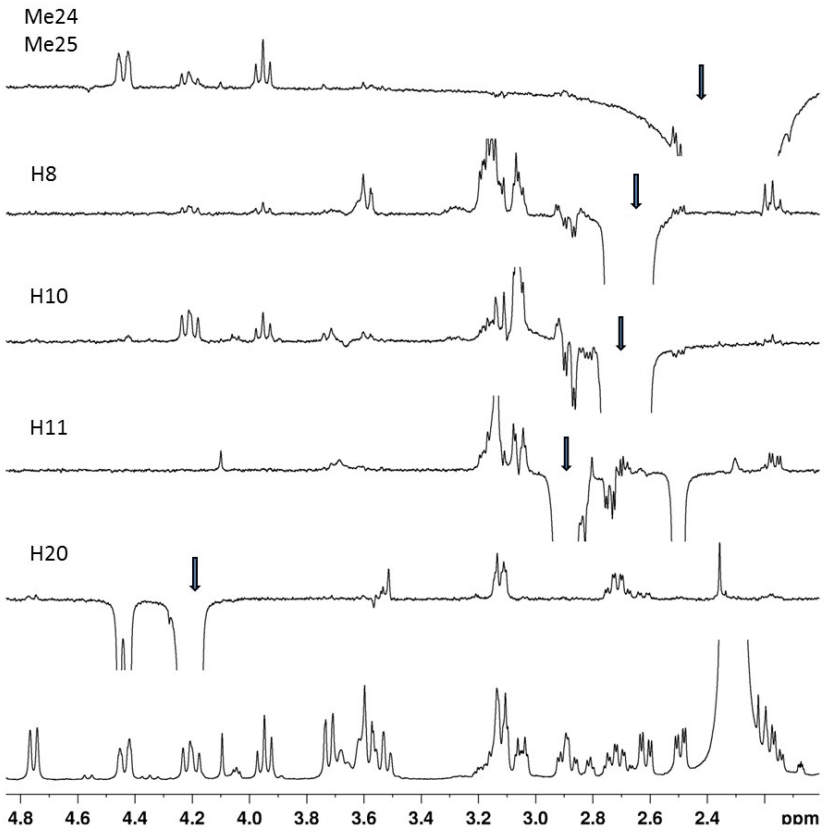

Figure S9. Series of noe 1D spectra of [**GaL^{pz*,NH}](ClO$_4$)** in CD_3CN. The irradiated protons are indicated. Strong negative peaks are due to saturation transfer.

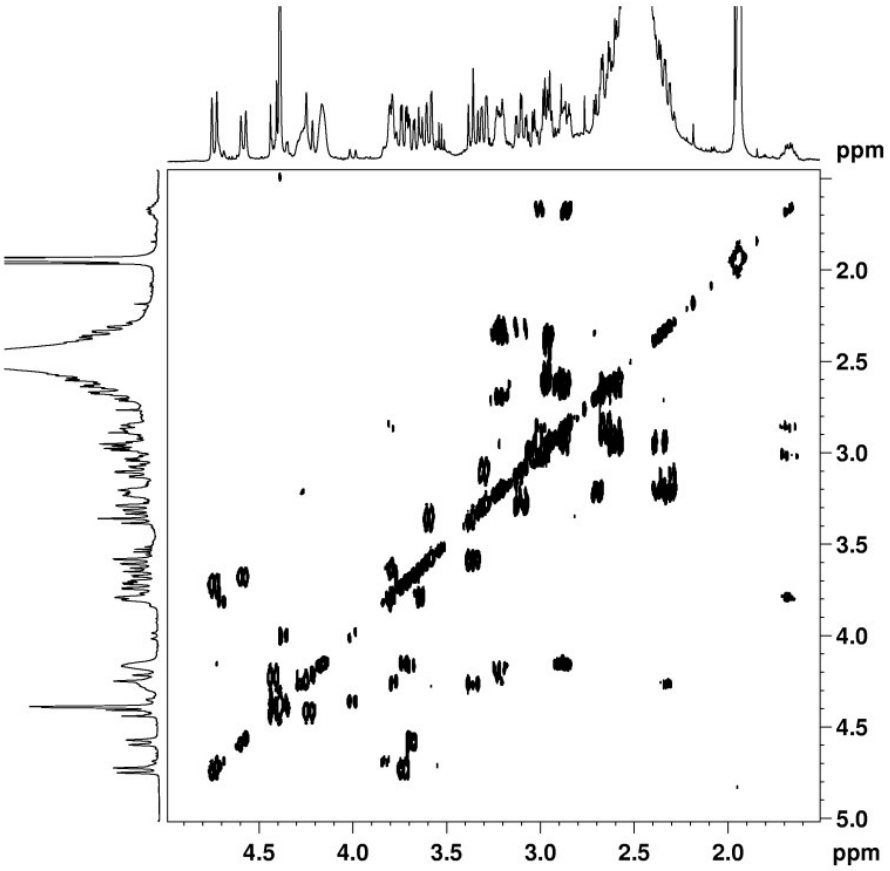

Figure S10. COSY spectrum of the methylenic protons of **[GaL^{py,NH}](ClO$_4$)** in CD_3CN.

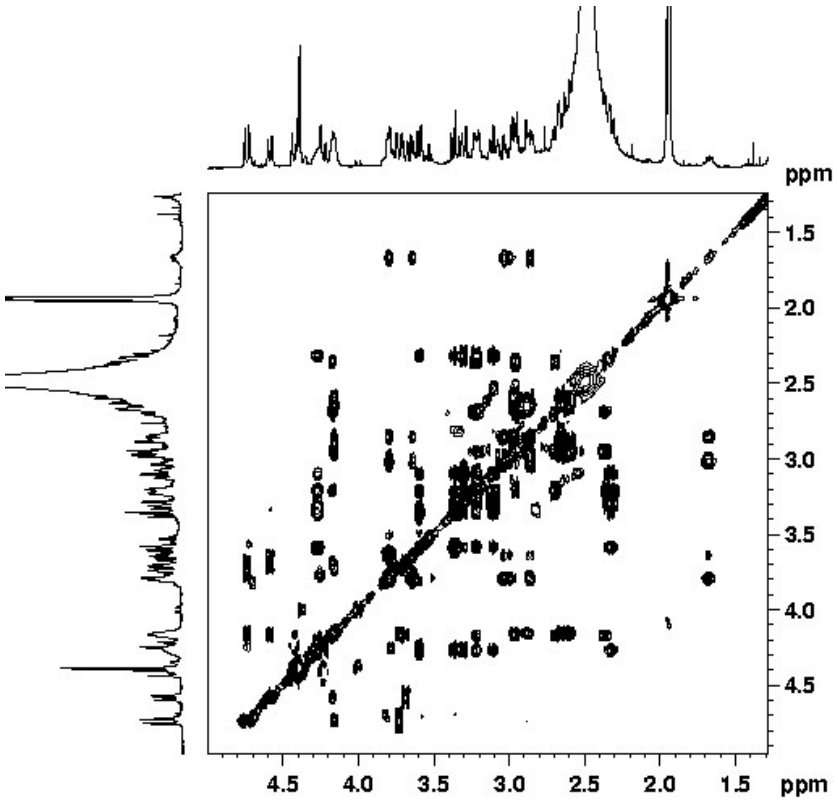

Figure S11. TOCSY spectrum of the methylenic protons of **[GaL^{py,NH}](ClO$_4$)** in CD_3CN.

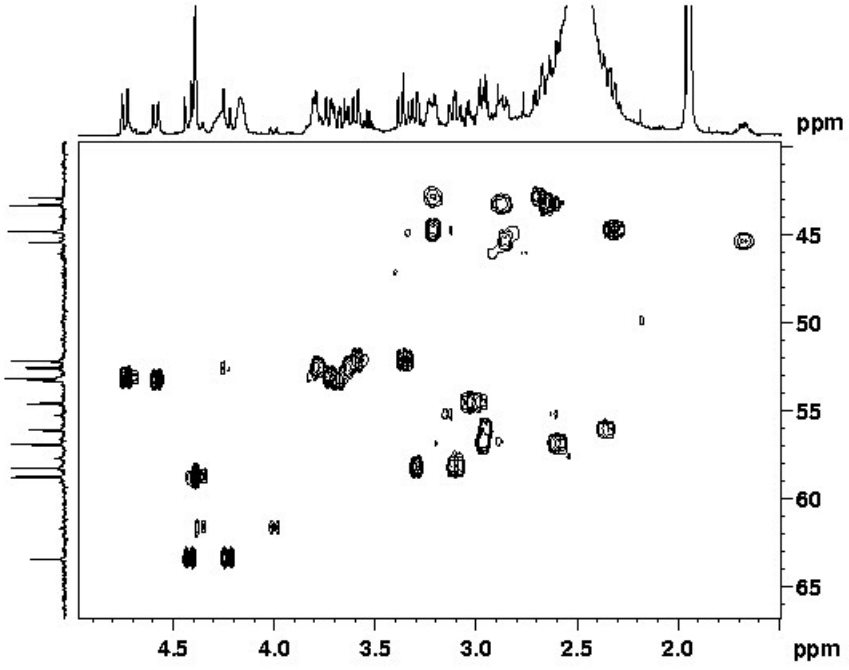

Figure S12. HSQC spectrum of the methylenic protons of **[GaL^{py,NH}](ClO$_4$)** in CD_3CN.

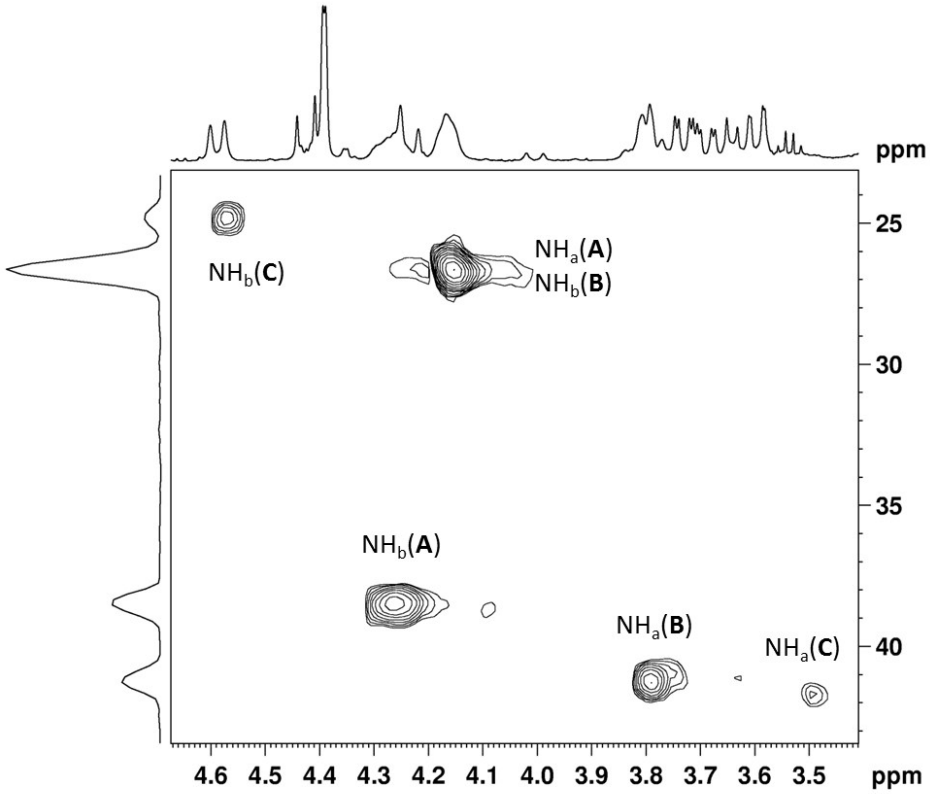

Figure S13. ^{1}H-^{15}N HSQC spectrum of [**GaL^{py,NH}](ClO$_4$)** in CD_3CN. The NH cross peaks of species A, B and C are assigned

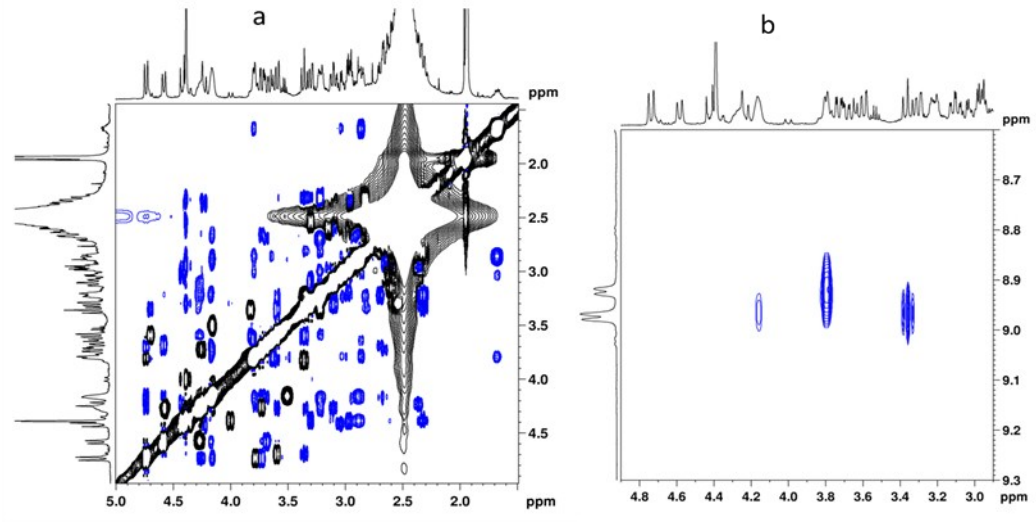

Figure S14 a) Crowded methylenic region of the NOESY spectrum of **[GaL^{py,NH}](ClO$_4$)** in CD_3CN. The spectrum is dominated by noe cross peaks of major species **A** and **B** in blue. The slow interconversion of species **A** and **C** gives rise to the exchange cross peaks (black peaks). The broad diagonal peak at around 2.5 ppm comes from residual water of the solvent. **b)** Aromatic region of the spectrum showing a long range noe between proton NH_a at 4.16 ppm and the *ortho* proton of the pyridyl ring in **A** at 8.97 ppm. In species **B** this proton is correlated with an axial CH_2 proton at 3.80 ppm from one of the phenolate-containing six-membered chelating ring.

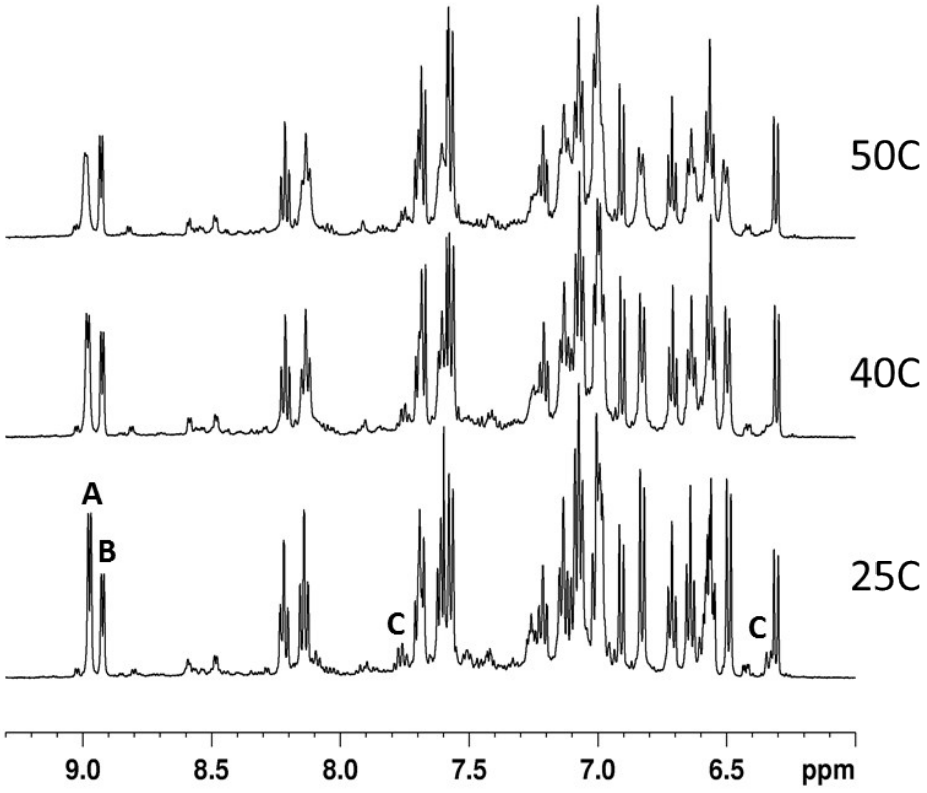

Figure S15. ^{1}H NMR of spectra of [**GaL^{py,NH}](ClO$_4$)** in CD_3CN at various temperatures, showing broadening of the signals for **A** and **C** as temperature is raised. Signals from isomer **B** remain sharp.

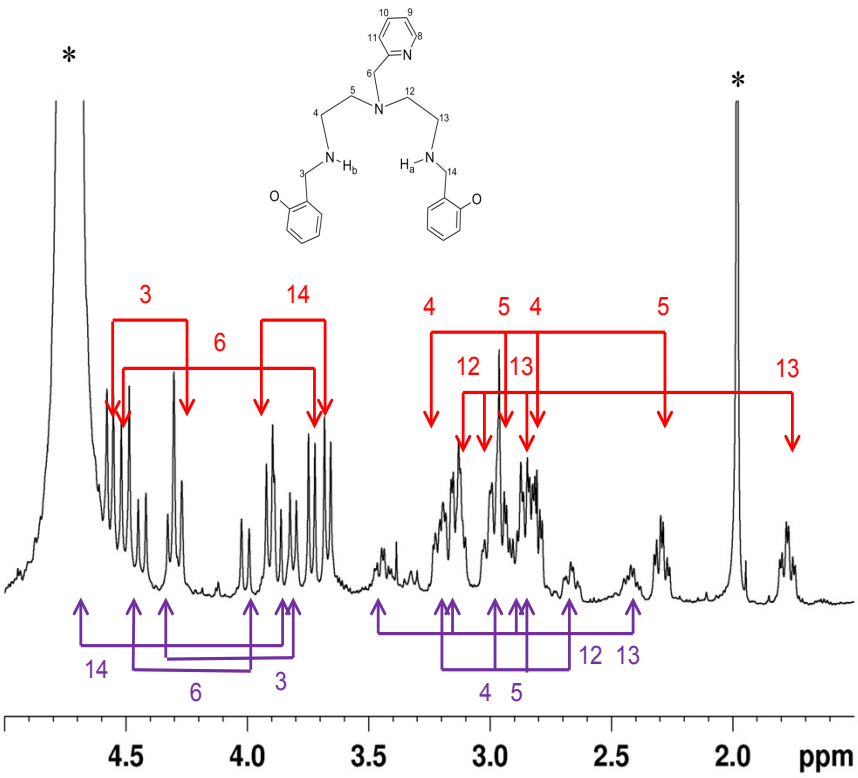

Figure S16. Aliphatic region of the ^{1}H spectrum of **[GaL^{py,NH}](ClO$_4$)** in D_2O showing the assignment of methylenic protons of **B** in red and **C** in magenta. Peaks from solvent and impurities are assigned by an *.

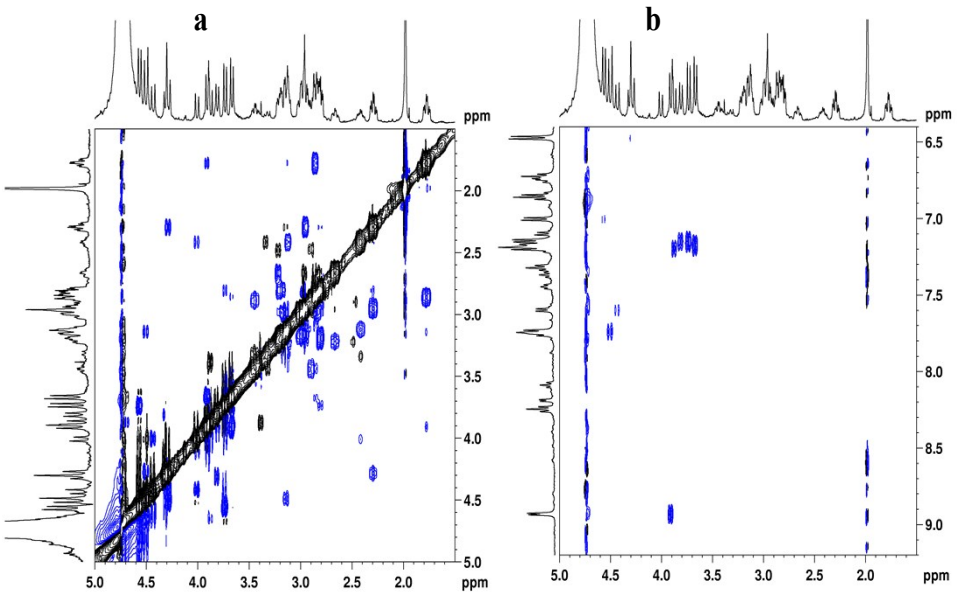

Figure S17 a) Crowded methylenic region of the NOESY spectrum of **[GaL^{py,NH}](ClO$_4$)** in D_2O. The spectrum is dominated by noe cross peaks of major species **B** and **C** in blue. The slow interconversion of species **A** and **C** gives rise to the exchange cross peaks (in black). **b)** Aromatic region of the spectrum. The *ortho* proton of the pyridyl ring in **C** at 8.19 ppm shows no long range noe correlations.

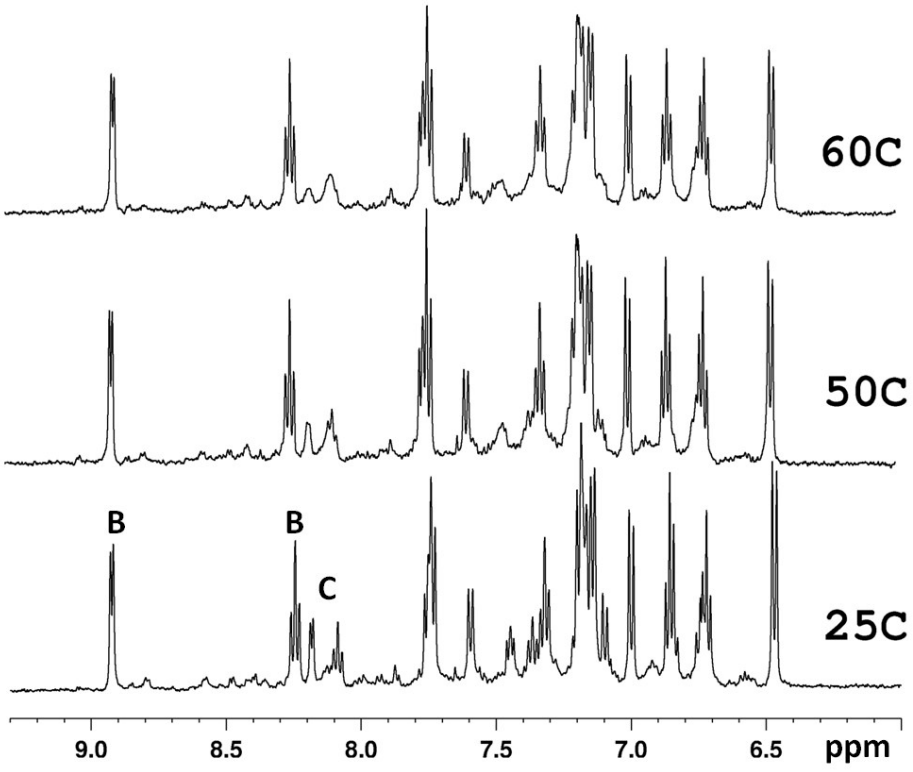

Figure S18. ^{1}H NMR of spectra of [**GaL^{py,NH}](ClO$_4$)** in D_2O at various temperatures, showing broadening of the signals for **C** as temperature is raised. Signals from isomer **B** remain sharp.

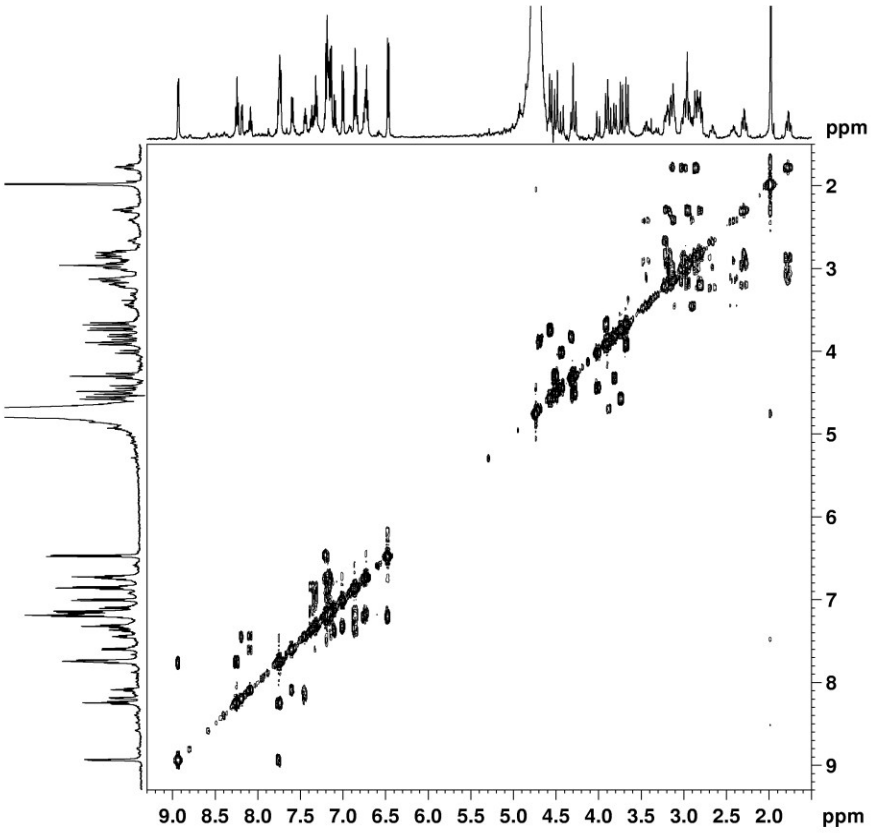

Figure S19. COSY spectrum of [**GaL^{py,NH}**]**(ClO_4)** in D_2O.

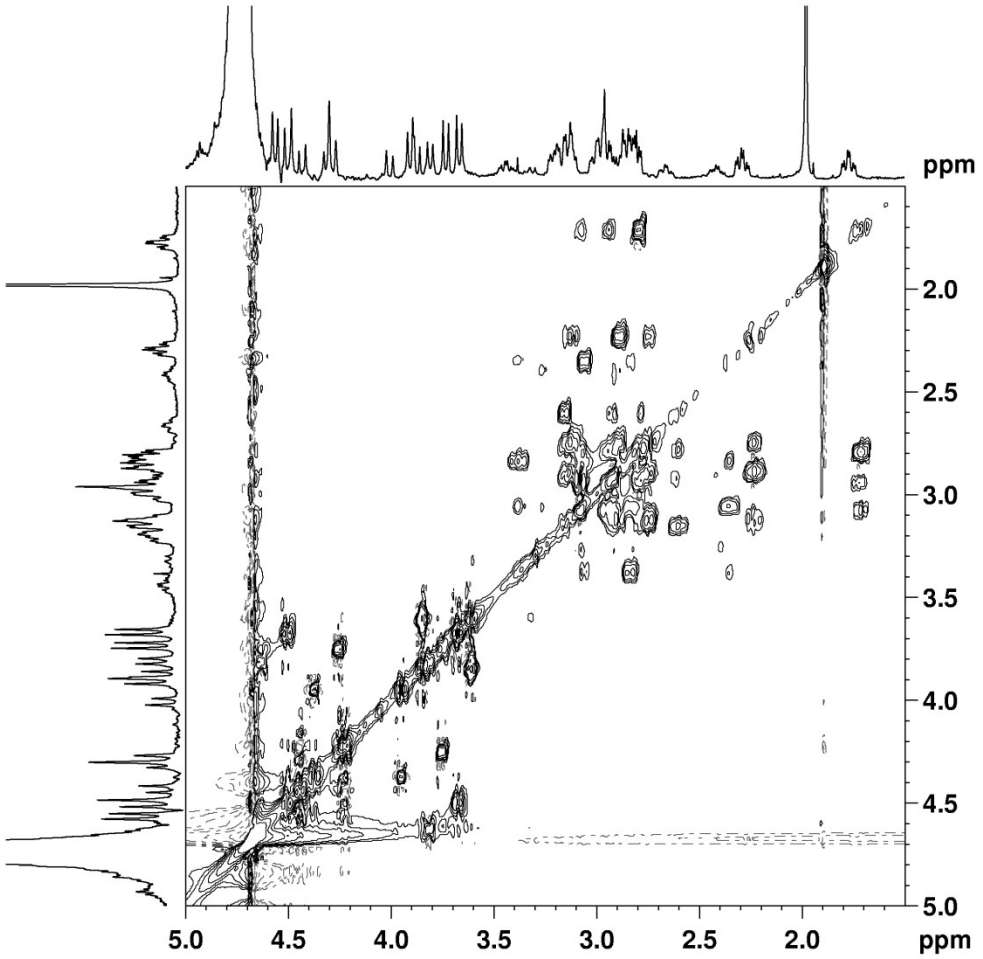

Figure S20. TOCSY spectrum methylenic protons of **[GaL^{py,NH}](ClO$_4$)** in D_2O.

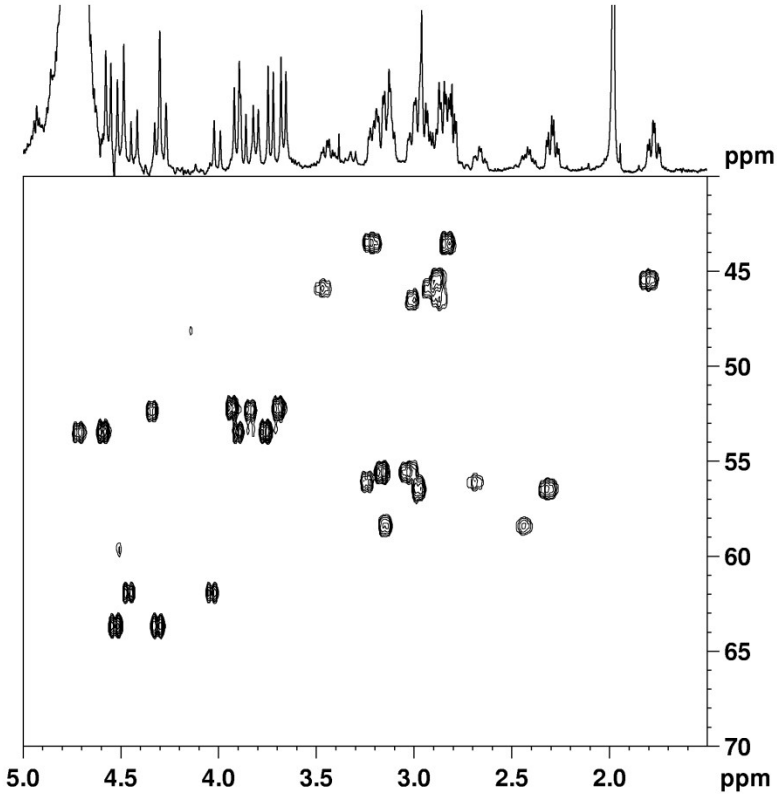

Figure S21. HSQC spectrum of the methylenic protons of [**GaL^{py,NH}](ClO$_4$)** in D_2O.

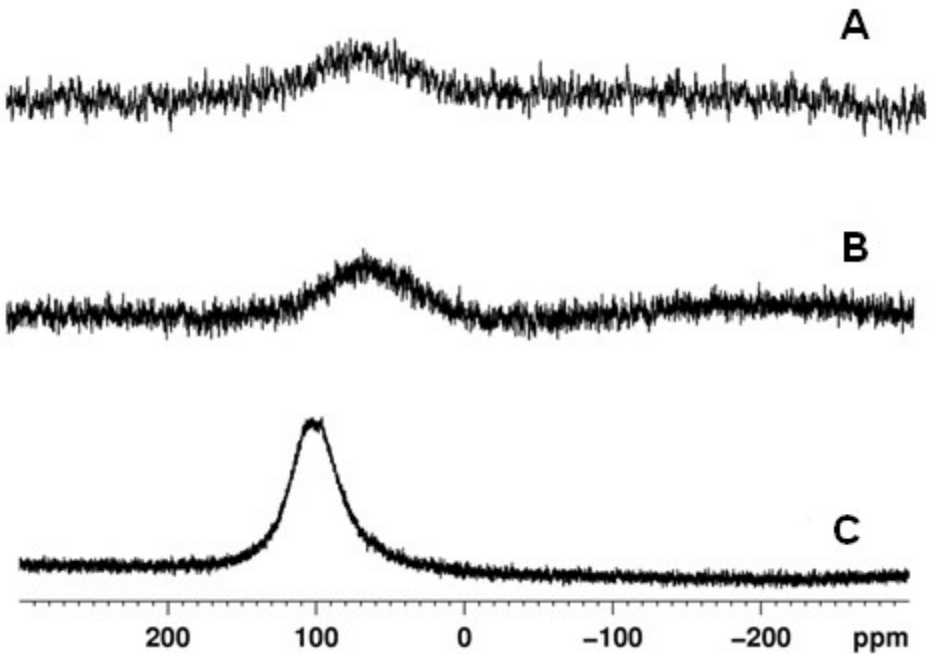

Figure S22. ^{71}Ga NMR of spectra of: **[GaL^{pz*,OMe}](ClO$_4$) (A)**, **[GaL^{pz*,NH}](ClO$_4$)** (**B**) and **[GaL^{py,NH}](ClO$_4$)** (**C**) in CD_3CN.

Biological studies

Table S3. Biodistribution results of $[^{67}GaL^{py,NH}]^+$ in female CD-1 mice expressed in %I.D./organ at 1 h and 4 h after i.v. administration.

Organ	% I.D./ Organ	
	1h	4 h
Blood	0.4 ± 0.2	0.4 ± 0.1
Liver	9.4 ± 2.5	7.3 ± 4.4
Intestine	48.6 ± 4.8	47.6 ± 9.2
Spleen	0.06 ± 0.01	0.03 ± 0.01
Heart	0.01 ± 0.00	0.01 ± 0.00
Lung	0.08 ± 0.02	0.05 ± 0.01
Kidney	1.2 ± 0.3	0.88 ± 0.06
Muscle	0.7 ± 0.2	0.39 ± 0.02
Skeletal	0.21 ± 0.04	0.27 ± 0.04
Stomach	0.11 ± 0.05	0.06 ± 0.03
Brain	< 0.01	0.01 ± 0.00
Excretion (% ID)	35.3 ± 2.4	41.9 ± 10.2

Table S4. Biodistribution results of $[^{67}GaL^{py,NH}]^+$ in female CD-1 mice expressed in %I.D./g at 1 h and 4 h after i.v. administration.

Organ	% I.D./ g Organ	
	1h	**4 h**
Blood	0.20 ± 0.08	0.20 ± 0.06
Liver	4.3 ± 1.4	4.3 ± 2.5
Intestine	13.2 ± 1.8	12.9 ± 2.6
Spleen	0.29 ± 0.1	0.18 ± 0.04
Heart	0.05 ± 0.01	0.07 ± 0.03
Lung	0.17 ± 0.02	0.14 ± 0.03
Kidney	2.3 ± 0.6	1.8 ± 0.2
Muscle	0.05 ± 0.01	0.03 ± 0.01
Skeletal	0.06 ± 0.02	0.08 ± 0.01
Stomach	0.14 ± 0.05	0.09 ± 0.04
Brain	0.02 ± 0.00	0.01 ± 0.00

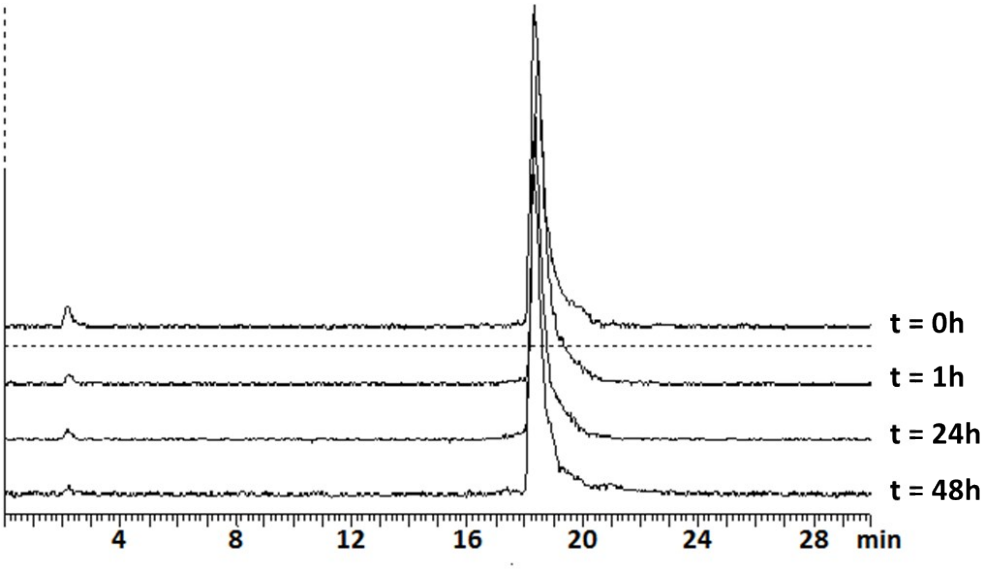

Figure S23. HPLC chromatograms of **[^{67}GaL^{py,NH}]$^{+}$** under challenge experiments with *apo*-transferrin after t = 0, 1, 24 and 48 h of incubation at 37 ºC.

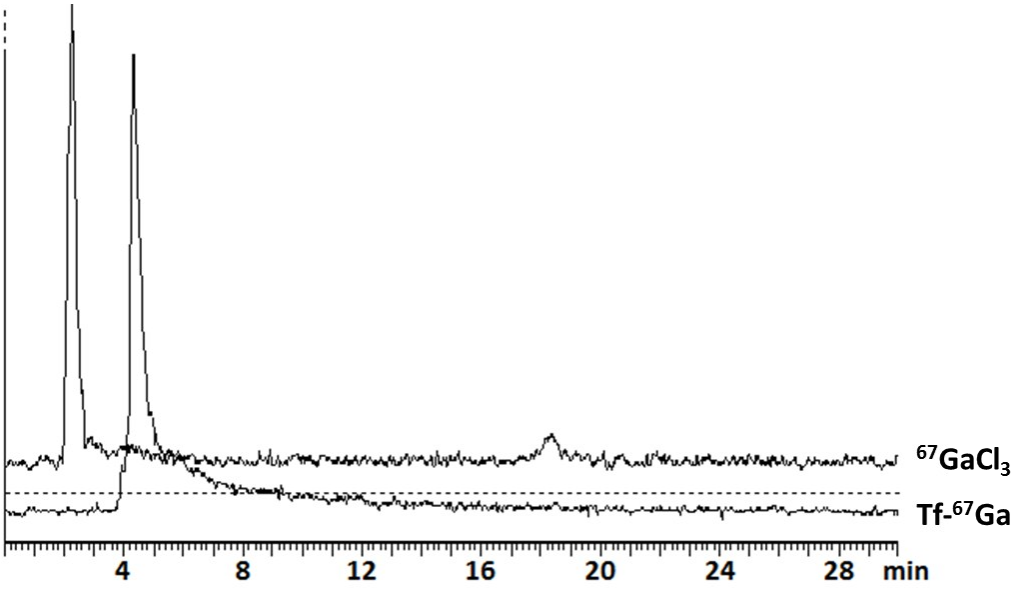

Figure S24. HPLC chromatograms of **$^{67}GaCl_3$** and **Tf-^{67}Ga.**

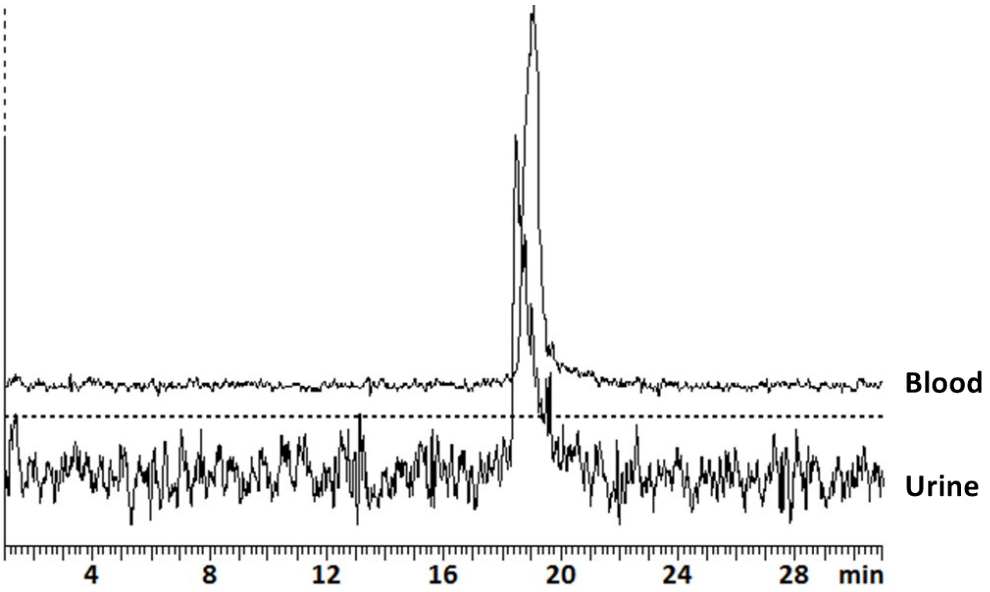

Figure S25. HPLC analysis of urine and blood from CD1-mice injected with **[^{67}GaL^{py,NH}]$^{+}$** at 4h post-injection.